

Fig. 3 Variation of wall temperature with coolant flow rate,  $T_0 = 539^\circ \text{K}$  ( $970^\circ \text{R}$ );  $P_0 = 207 \text{ N/cm}^2$  (300 psia);  $m_\infty^0 = 4.1 \text{ kg/sec}$  (9.0 lb/sec);  $u_\infty^0 = 11.0 \text{ m/sec}$  (36.1 ft/sec).

and at  $z = 10.4 \text{ cm}$  (4.1 in.). These hot spots are possibly the result of extreme mixing caused by the low main stream velocity relative to the coolant injection velocity ( $u_\infty^0/u_c = 0.23$ ) or flow separation. Similar hot spots were noted when the pipe inlet was rotated  $180^\circ$  relative to the nozzle indicating that nonuniformities in the flow pattern at the slot were probably not responsible for this behavior.

The decrease in wall temperature with increasing coolant flow rate appears to reach an optimum as shown in Fig. 3. At nearly all of the stations, a large reduction in wall temperature occurs in the coolant flow range of  $0 < m_c/m_\infty^0 < 0.02$ . At higher values of  $m_c/m_\infty^0$ , the reduction in wall temperature is small and in some cases, the wall temperature actually increases (hot spots at  $m_c/m_\infty^0 = 0.10$ ). The velocity ratio  $u_\infty^0/u_c$  corresponding to the optimum reduction in wall temperature is approximately 1.0; that is, the optimum injection velocity appears to be equal to or possibly slightly greater than the main stream velocity.

### Summary

The results of the present experimental study in a cooled  $30^\circ$  half angle of convergence nozzle tend to be consistent with the results of Ref. 3 which indicated 1) the feasibility of using a modified effectiveness  $\eta'$  to correlate film cooling in non-adiabatic wall accelerated flows provided the main stream to coolant velocity ratio at the slot is about 1.0, and 2) that a main stream to coolant velocity ratio of about 1.0 provides the optimum cooling effectiveness. A slight improvement in the correlation of Ref. 3 was obtained by using local rather than slot conditions in the evaluation of  $\phi$ . It should be recognized that the results of this study were based on a single set of main stream flow conditions and geometric parameters. Therefore, extrapolation to other conditions must await further verification.

### References

- Hatch, J. E. and Papell, S. S., "Use of a Theoretical Flow Model to Correlate Data for Film Cooling or Heating an Adiabatic Wall by Tangential Injection of Gases of Different Fluid Properties," TN D-130, 1959, NASA.
- Lucas, J. G. and Golladay, R. L., "Gaseous-Film Cooling of a Rocket Motor with Injection Near the Throat," TN D-3836, 1967, NASA.
- Lieu, B. H., "Air-Film Cooling of a Supersonic Nozzle," NOLTR 64-65, Aug. 1964, Naval Ordnance Lab., White Oak, Md.
- Seban, R. A. and Back, L. H., "Effectiveness and Heat Transfer for a Turbulent Boundary Layer with Tangential Injection and Variable Free-Stream Velocity," *Journal of Heat Transfer*, Vol. 84, No. 3, Aug. 1962, pp. 235-244.
- Beckwith, I. E. and Bushnell, D. M., "Calculation by a Finite-Difference Method of Supersonic Turbulent Boundary Layers with Tangential Slot Injection," TN D-6221, 1971, NASA.
- Boldman, D. R., Neumann, H. E., and Schmidt, J. F., "Heat Transfer in  $30^\circ$  and  $60^\circ$  Half-Angle of Convergence Nozzles with Various Diameter Uncooled Pipe Inlets," TN D-4177, NASA.

## Parameters Influencing Dynamic Stability Characteristics of Viking-Type Entry Configurations at Mach 1.76

CHARLES H. WHITLOCK\* AND PAUL M. SIEMERS III†  
NASA Langley Research Center, Hampton, Va.

### Nomenclature‡

- $C_m$  = pitching moment coefficient  
 $C_{mq}$ ,  $C_{m\dot{\alpha}}$  =  $\partial C_m / \partial (qD/2V)$ ,  $\partial C_m / \partial (\dot{\alpha}D/2V)$ , ( $\text{rad}^{-1}$ )  
 $d_s$ ,  $D$  = sting diameter, model diameter, m  
 $l_s$  = sting length, m  
 $R_N$  = Reynolds number  
 $V$  = freestream velocity, m/sec  
 $\alpha$  = angle of attack, deg  
 $\theta$  = balance oscillation amplitude, deg  
 $\omega$  = body oscillation frequency, rad/sec

### Introduction

BLUNT conical configurations have been considered for Entry vehicles because of their high-drag characteristics. Early tests<sup>1</sup> discovered that such configurations may be dynamically unstable in the transonic speed range; however, results were inconsistent. Other tests<sup>2,3</sup> defined angle of attack as one parameter which might explain the inconsistencies, and forced-oscillation tests<sup>4,5</sup> were conducted to define the extent of nonlinearity with angle of attack.

Additional inconsistencies were uncovered by the forced oscillation data. A number of parameters may contribute to the inconsistencies. The effects of Reynolds number, reduced frequency parameter, and tunnel vibration were not understood, and data at low angles of attack were inconsistent for similar configurations when model size was changed. Attempts to simulate the motions of a full-scale flight vehicle with the tunnel data were unsuccessful. Applicability of data from in-plane forced-oscillation techniques to predict flight motions which cross the angle-of-attack plane (elliptic or conical motions) was questioned. It was also realized that the forced-oscillation data were average (or effective) values over a small amplitude range about a nominal angle of attack but motion studies require values based on the instantaneous angle of attack. The effect of changes in base geometry was also a question. Some results<sup>4,5</sup> indicated minimum effects although other data<sup>6</sup> showed that the transonic instability could be completely eliminated by proper selection of base geometry.

A two-part investigation was initiated to define the important variables which influence the transonic dynamic stability characteristics of blunt-conical configurations. Free-oscillation tests of three Viking-type configurations were conducted in Tunnel A of the von Kármán Gas Dynamics Facility at the Arnold Engineering Development Center. A parallel effort developed a technique for correcting either forced- or free-oscillation damping data to values based on the instantaneous angle of attack. This note will briefly summarize the results of these investigations using Mach 1.76 results.

### Wind-Tunnel Results

The configurations tested in the Tunnel A facility are shown in Fig. 1. Model 721 is an early proposed design from which the present VIKING configuration was derived. It is the only configuration of this series which had been subject to previous

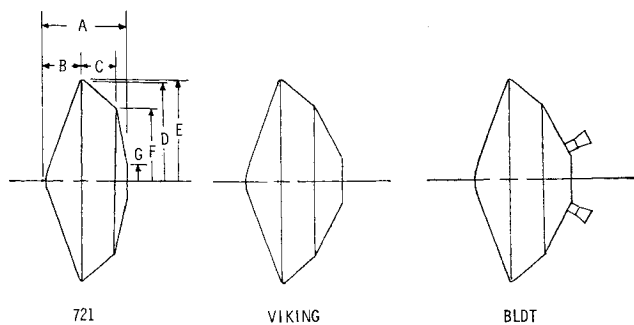
Received January 17, 1972; revision received March 20, 1972.

Index categories: Spacecraft Attitudes Dynamics and Control; Entry Vehicle Dynamics and Control; Nonsteady Aerodynamics.

\* Aerospace Engineer. Member AIAA.

† Aerospace Engineer.

‡ Dots over symbols indicate derivatives with respect to time.



CONFIGURATION	A	B	C	D	E	F	G
721	0.412D	0.187D	0.163D	0.50	0.514D	0.36D	0.0925D
VIKING	0.488D	0.184D	0.167D	0.50	0.5025D	0.368D	0.109D
BLDT	0.488D	0.184D	0.167D	0.50	0.5025D	0.368D	0.109D

NOSE RADIUS = 0.25D

Fig. 1 Configurations tested in Tunnel A.

tests.<sup>4,5</sup> The BLDT configuration is to be used during qualification tests of the VIKING decelerator and is identical to VIKING except for protuberances of rocket motor nozzles from the base.

Tests of the 721 configuration were used to compare Tunnel A results with previous Propulsion Wind Tunnel (PWT) data.<sup>4,5</sup> Mach number, Reynolds number, reduced-frequency parameter, and sting length ( $l_s/D = 1.30$ ) were similar, but sting diameter was not matched. The free oscillation data ( $d_s/D = 0.183$ ) from the relatively smooth Tunnel A facility agreed with the forced oscillation results from the transonic PWT facility ( $d_s/D = 0.097$ ).

The effects of sting geometry for blunt conical configurations are shown in Fig. 2. Effective  $C_{mq} + C_{m\dot{a}}$  values are based on an oscillation  $\theta = \pm 1.8^\circ$ , and symbol size is indicative of scatter in the test results. Figure 2a shows that damping values at low angle of attack are influenced by sting diameter, and Fig. 2b indicates a large variation with sting length. Sting geometry requirements for the elimination of

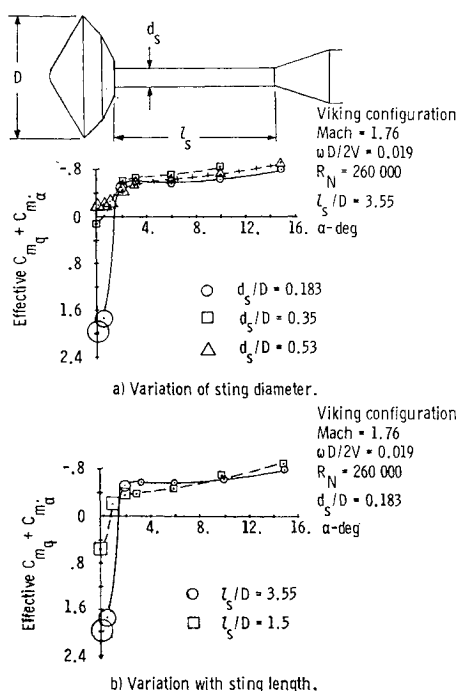


Fig. 2 Effects of sting geometry.

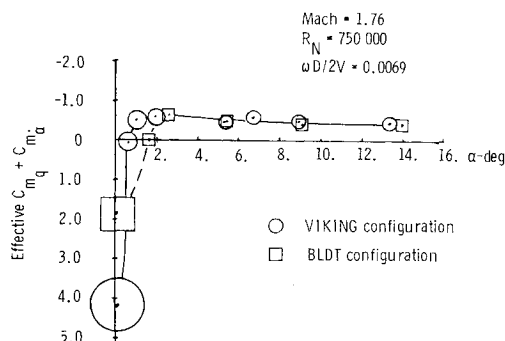


Fig. 3 Effects of configuration geometry.

sting effects have not been established. Data at higher Mach numbers indicate negligible sting effects.

The effects of configuration base geometry changes are shown in Fig. 3. When all test parameters are matched, changes in base geometry had a significant effect on low angle-of-attack dynamic stability coefficients. Other data from these tests indicate that base geometry effects diminish at higher supersonic velocities.

Cross plane data were compared with in-plane damping values. Within the scatter of the data, the results were in agreement. This indicates that it is valid to use conventional in-plane oscillation data to predict conical or elliptic motions of blunt conical spacecraft.

The effects of Reynolds number and reduced-frequency parameter are shown in Figs. 4 and 5. Only at both low angle of attack and low values of the reduced-frequency parameter is there a significant Reynolds number effect. At all Reynolds numbers, there is a significant reduced-frequency effect only at low angles of attack. It is unknown whether these results are influenced by sting geometry.

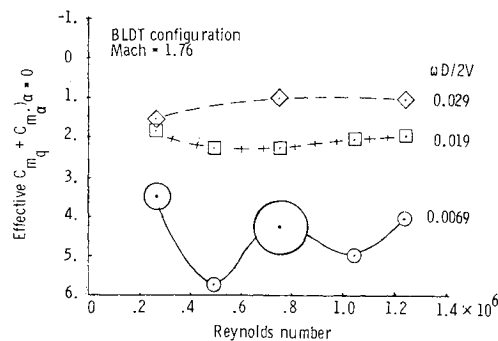


Fig. 4 Effects of Reynolds number.

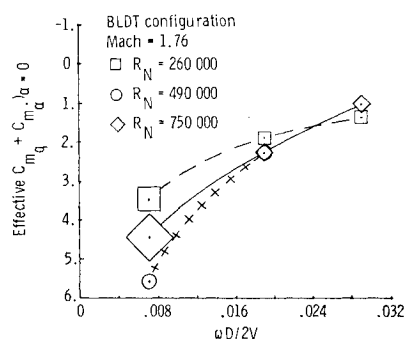


Fig. 5 Effects of reduced-frequency parameter.

### Nonlinear Correction

Computer simulated motion studies require damping coefficient values based on the instantaneous (or local) angle of attack. Both the forced-oscillation and free-oscillation techniques produce damping coefficients that are average or effective values over the oscillation amplitude about the nominal angle of attack. When the damping coefficient is constant with angle of attack, the effective value is equal to the value based on instantaneous angle of attack. When the data are nonlinear with angle of attack, a procedure to extract an instantaneous damping coefficient curve from the experimental effective values is required. A procedure to correct for nonlinearity in either forced-or-free-oscillation data has been developed at the Arnold Engineering Development Center.<sup>7</sup> The technique is applied here to certain of the effective damping data shown previously. Figure 6 is a typical example showing the effects of the correction. It is evident that the nonlinear correction can be significant and must be applied prior to computer motion studies when the data are nonlinear. For blunt conical configurations of the Viking type, it appears essential that the correction be applied when anticipated motions may pass near zero angle of attack.

### Conclusions

A two-part investigation has been conducted to define the important variables which influence the dynamic stability characteristics of blunt conical configurations. From results of the investigation, the following conclusions are made: 1) The effects of sting geometry are significant in the low angle-of-attack range; 2) Variation of the reduced-frequency parameter and model base geometry caused significant effects in the data. Reynolds number also was significant at low values of the reduced-frequency parameter; 3) The effects of cross plane motions and tunnel vibration characteristics appear negligible. Free-oscillation data from the VKF-Tunnel A facility agreed with forced-oscillation results from the PWT-16T facility when all test environment parameters except sting diameter were matched. The diameter ratios were small, however, diameter effects are not completely understood for small sizes; and 4) An approximate technique has been developed to convert effective data from either forced-oscillation or free-oscillation tests to values based on the instantaneous angle of attack.

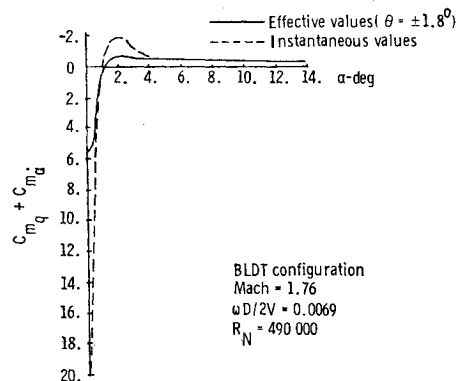


Fig. 6 Effect of typical nonlinear correction.

### References

- 1 Krumins, M. V., "Drag and Stability of Mars Probe/Lander Shapes," *Journal of Spacecraft and Rockets*, Vol. 4, No. 8, Aug. 1967, pp. 1052-1057.
- 2 Whitlock, C. H., Bendura, R. J., and Henning, A. B., "Damping Derivatives of 120° Conical Spacecraft from Flights in a Low-Density Environment," *Journal of Spacecraft and Rockets*, Vol. 6 No. 8, Aug. 1969, pp. 937-939.
- 3 Marko, W., "Dynamic Stability of High-Drag Planetary Entry Vehicles at Transonic Speeds," *Journal of Spacecraft and Rockets*, Vol. 6 No. 12, Dec. 1969, pp. 1390-1396.
- 4 Uselton, B. L., Shadow, T. O., and Mansfield, A. C., "Damping-In-Pitch Derivatives of 120- and 140-Deg Blunted Cones at Mach Numbers from 0.6 through 3," TR-70-49, April 1970, Arnold Engineering Developing Center, Arnold Air Force Base, Tullahoma, Tenn.
- 5 Steinberg, S., "Experimental Pitch Damping Derivatives for Candidate Viking Entry Configurations at Mach Numbers from 0.6 to 3.0," TR-3709005, June 1970, Martin Marietta Corp., Baltimore, Md.
- 6 Sammonds, R. I., "Transonic Static-and Dynamic-Stability Characteristics of Two Large-Angle Spherically Blunted High-Drag Cones," AIAA Paper 70-564, Tullahoma, Tenn., 1970.
- 7 Billingsley, J. P. and Norman, W. S., "Relationship Between Local and Effective Nonlinear Aerodynamic Pitch-Damping Derivatives as Measured by a Forced-Oscillation Balance for Preliminary Viking Configurations," TR-72-25, March 1972, Arnold Engineering Developing Center, Arnold Air Force Base, Tullahoma, Tenn.